Petroleum and Coal

Article **Open Access**

Modeling and Investigation of the Operational Parameters in the Process of Mercaptan and Water Removal from Natural Gas by Adsorption on Zeolite 13X

Jafar Sadeghzadeh Ahari[1], Zahra Shafiee[1], Khashayar Mohammadbeigy[1], Saeed Pakseresht[2], Majid Kakavand [1], Mehdi Kolivand[1]

[1] *Gas Department-Research Institute of Petroleum Industry, Tehran, Iran*
[2] *R&T Management of National Iranian Gas Company, Tehran, Iran*

Received April 4, 2016; Accepted June 8, 2016

Abstract

In this study an industrial demercaptanization unit having a molecular sieve 13X as an absorbent has been modeled by mathematical equations of mass, energy and momentum. In this modeling, linear driving force approximation has been used for calculation of adsorption rate. Moreover, the Langmuir isotherm developed grade 2 relation has been used to express the equilibrium conditions of water and mercaptan concentration in gas and solid phases. After validation of the modeling results with those of the experimental data, the effects of the operational parameters such as adsorbent diameter, regeneration gas flow rate, feed pressure and feed temperature on water and mercaptan content of the unit product has been investigated.

Keywords: Demercaptanization; Modeling; Zeolite 13X; Operating Parameters.

1. Introduction

Mercaptan is a conventional term used for sulfur compounds with -SH functional group. These substances are naturally found in sour gas, coal tar and gas condensates. Having a highly unpleasant odor, especially in light mercaptan (methyl and ethyl mercaptan), is one of their main recognition characteristics.

Existence of sulfur compounds such as mercaptan and hydrogen sulfide in gas leads to serious problems such as health risk, deactivation of metal and metal oxide catalysts in different processes and corrosion in process equipment and pipelines. On the other hand, the combustion of gases containing sulfur compounds produces sulfur dioxide whose excessive accumulation in the environment causes problems such as respiratory disorders and acid rains leading to so many environmental impacts.

Due to these hazardous environmental impacts, different processes have been proposed to remove mercaptan components from gas streams. There are two typical and conventional processes addressed in industry for this purpose i.e. Merox and gas adsorption by solid adsorbent. In first process (Merox), mercaptan is separated by a caustic solution and in second approach; mercaptan components are removed through Pressure-Temperature Swing Adsorption (PTSA) process by passing the gas on an activated solid bed [1].

Since mercaptan adsorption is an exothermic process, increase of the temperature will decrease the adsorption rate. So, adsorption is carried out at low temperature until the equilibrium condition is reached. At this point in time, no further adsorption capacity is available and the adsorbent material must be regenerated. The regeneration is achieved by increase of the adsorption bed temperature which can take place by applying heat to the bed or more commonly by purging a portion of the product at high temperature. The limitation in Temperature Swing Adsorption (TSA) process is the regeneration time. As heating or cooling of the bed during regeneration is a slow process, the time duration of each TSA cycle usually

ranges from several hours to over a day. This time delay makes TSA unsuitable for rapid cycling processes [2]. Thus, there is a need modification for temperature swing adsorption processes that having faster cycle times, while maintaining or improving the final product stream purity. This modification is combination of two main adsorption processes (TSA and PSA) and it is called Pressure-Temperature Swing Adsorption (PTSA) process. In this process, unlike TSA process the pressure is lowered before heat is applied.

In PTSA processes used for adsorption of mercaptan, the adsorption is carried out at temperature of 20-60°C and the regeneration takes place at 200-350°C. The most important adsorbents used for mercaptan adsorption are metal reinforced zeolites and activated carbon. Active carbon has a higher adsorption capacity in compare with zeolites but its application has been limited because of having temperature sensitivity. Therefore, zeolite is widely used as an adsorbent in current industrial demercaptanization units.

Wakita *et al.* [3] studied the adsorption of di-methyl di-sulfide (DMS) and t-butyl mercaptan (TBM) from natural gas in vicinity of Na-Y, Na-X and Ca-X zeolites. The results showed that Na-Y zeolite had a higher adsorption capacity than the other ones [3].

The adsorption of impurities such as ethyl mercaptan, normal heptane and toluene by Na-X adsorbent has been investigated by Weber *et al.* [4]. It has been shown that Na-X adsorbs better ethyl mercaptan than the others components. Tamai *et al.* [5] studied the effects of carbon activation on methyl mercaptan adsorption by treating activated carbon with application of HNO_3/H_2SO_4 acid mixture, heating of that in argon atmosphere and adsorption of cethylamine. The results showed that acid washing was more efficient than the other methods for increase of adsorption capacity. It has also been shown in this study that increase of the sulfuric acid ratio in $HNO_3/H2SO_4$ solution leads to increase of the adsorption capacity. It has been reported in their study that hydrogen bonding between acidic groups formed by acid-treatment and thiol groups of methyl mercaptan causes increase in adsorption of methyl mercaptan on activated carbon.

Mathematical modeling, although very much useful for design and optimization of various processes, has been rarely addressed for demercaptanization process in literature. Esmaili & Ehsani [6] and Shirani *et al.* [7] have modeled gas demercaptanization process by zeolite 13X. In these researches, only the adsorption step has been modeled and the effects of various parameters such as feed pressure, feed composition and bed height have been investigated on adsorption curve.

As the PTSA process consists of two consecutive steps, i.e. adsorption and regeneration, it would be necessary to study both steps simultaneously as a complete cycle. In this study, to somehow complete Esmaili & Ehsani [6 and Shirani *et al.* [7] works, the complete cycle of PTSA process has been modeled and then the effects of operational parameters on adsorption performance have been investigated.

2. Process description

The unit under study contains six beds with 13X zeolite adsorbent. During the operation, three beds are on-stream at high pressure for separating the impurities from process feed (adsorption mode), while the other three beds are working at lower pressure and high temperature for regeneration mode. The total cycle time is 36 hours comprising of 6 steps. In first step, adsorption is performed by passing the gas across the bed in 18 hours to remove its mercaptan and water contents. After this step, the bed is saturated so it should be regenerated. Regeneration or desorption time is 17 hours. In this mode, the pressure of adsorption column is decreased from 67 barg to 10 barg in 30 minutes. During first stage of regeneration step, a slip stream of the clean dry gas about 5.5 volume percent passes to the regeneration gas heater and then enters into the bed to increase its temperature from 20°C to 180°C. The required time for this stage is six hour. At the next heating stage, temperature of the bed increases from 180°C to 290°C. This stage also needs 6 hours. At the next stage, for recovering of the operating conditions, the bed is cooled down for 4 hours and its temperature decreases from 290 to 20°C to maintain the required operation temperature. At

the last stage of regeneration step, the bed is pressurized for 30 minutes from 10 barg to 67 barg. After about an hour rest, the bed goes to adsorption step. The mercaptan content in the product stream of the mentioned industrial unit is reported to be 15 mg/Nm^3 (5 ppmv).

The bed dimensions as well as feed specifications are illustrated in tables 1 and 2 respectively.

Table 1. Bed and adsorbent specification

Bed specification	
Length (mm)	4650
Internal Diameter (mm)	3750
Porosity	0.36
Adsorbent specification	
Diameter (mm)	3
Heat capacity (J kg^{-1} K^{-1})	1000
Porosity	0.37
Bulk Density (kg/m^3)	650

Table 2. Gas feed specification

Inlet condition			
Temperature (K)		293.15	
Pressure (barg)		67	
Flow rate (kmol/h)		7956	
Feed component (mol %)			
Methane	86.344	Methyl Cyclo Pentane (MCP)	0.0017
Ethane	5.46	Benzene	0.001
Propane	2.17	n-Hexane	0.023
i-Butane	0.3785	N_2	3.58
n-Butane	0.5125	CO_2	1.33
i-Pentane	0.1088	Mercaptan	0.00107
n-Pentane	0.088	H_2O	0.0018

3. Mathematical model

To understand the dynamic behavior of a TSA process, a mathematical model is needed to incorporate mass, momentum and energy balances over a packed bed with appropriate boundary conditions for each step of the TSA cycle.

3.1. Assumptions

In order to develop a dynamic model for this system, the following assumptions are introduced:

- Gas stream behavior follows Peng-Robinson state equation (for calculation of Z Factor) [8].
- The bed has been considered to be one dimensional (In the longitudinal direction).
- The pressure drop along the bed is estimated by Ergun equation [8].
- The fluid flow is described by an axially dispersion plug flow model.
- The concentrations of the adsorbed and gas phases inside adsorbent particles are assumed to be lumped.
- Constant porosity has been considered along the bed.
- The mass transfer rate is represented by linear driving force (LDF)
- Thermal equilibrium has been assumed between adsorbents and fluids.
- The column wall interchanges energy with gas phase inside the column and heat transfer between the bed wall and environment is ignored (Adiabatic).
- The gas feed contains more than 10 components, but adsorbent 13X has a tendency to adsorb only polar materials such as mercaptan and water [7]. So other components are

considered to be inert. In other word the feed is considered to have three components: water, mercaptan and inert. In this study, the third component is considered to be methane (summation of all components except for water and mercaptan).

- Considering the short time of depressurizing and pressurizing steps compared with those of adsorption and regeneration, the concentration and temperature variations during these steps have been ignored and just a linear relation has been incorporated to calculate pressure variations against time.

3.2. Material Balance

According to the assumed assumptions, the behavior of the system has been described by the following set of equations:

3.2.1. Mass balance for each component of the gas phase

$$\frac{\partial C_i}{\partial t} = D_{z,i}\frac{\partial^2 C_i}{\partial Z^2} - U\frac{\partial C_i}{\partial Z} - C_i\frac{\partial U}{\partial Z} - \left(\frac{1-\varepsilon}{\epsilon}\right)\rho_p\frac{\partial q_i}{\partial t} \quad (1)$$

3.2.2. Overall mass balance for the gas phase

$$C_t\frac{\partial U}{\partial Z} + \frac{1-\varepsilon}{\varepsilon}\rho_p\sum_{i=1}^{n}\frac{\partial q_i}{\partial t} = 0 \quad (2)$$

3.2.3. Mass balance for the solid phase

The rates of mass transfer in adsorption processes are determined by some mathematical equations in form of $\frac{\partial \mathrm{q}}{\partial \mathrm{t}}$ to estimate the transfer rates of the components from the gas phase to the solid phase (sorbent). Generally, there are three basic models to determine the rates of mass transfer in adsorption processes:

- Induced Pore-Diffusion
- Linear Driving Force (LDF)
- Based Equilibrium

As already mentioned, Linear Driving Force model has been used in this study. Based on this model, the diffusion rates of the components are calculated by the following equation:

$$\frac{\partial \mathrm{q_i}}{\partial \mathrm{t}} = \mathrm{K_{s,i}}(\mathrm{q_i^*} - q_i) \quad (3)$$

3.3. Energy balance

PTSA is a non-isothermal process. To model this process, besides mass and momentum balance equations, the energy balance should be considered as well.

$$\frac{\partial T}{\partial t} = \frac{1}{\rho_g c_{pg} + \frac{(1-\varepsilon)}{\varepsilon}\rho_p c_{ps}}\left[\lambda\frac{\partial^2 T}{\partial Z^2} - \rho_g c_{pg} U\frac{\partial T}{\partial Z} - \rho_g c_{pg} T\frac{\partial U}{\partial Z} + \rho_p\frac{1-\varepsilon}{\varepsilon}\sum H_i\frac{\partial q_i}{\partial t}\right] \quad (4)$$

3.4. Momentum balance

As already declared, the pressure drop across the bed is calculated by Ergun equation:

$$\frac{\partial P}{\partial Z} = -\left(\frac{1.5\times10^{-3}\mu(1-\varepsilon)^2 U}{d_p^2\varepsilon^3} + \frac{1.75\times10^{-5}\rho_g(1-\varepsilon)U^2}{d_p\varepsilon^3}\right) \quad (5)$$

3.5. Boundary and Initial Conditions

PTSA cycle is a sequence of elementary steps. To properly simulate a PTSA process, the conservation equations presented earlier should be coupled with the appropriate boundary and initial conditions for each step. The boundary conditions associated with adsorption and regeneration steps are presented as following:

3.5.1. Adsorption Step

In a cyclic operation, the initial conditions for each step are the conditions at the end of the previous step. For startup a clean bed has been assumed. Therefore for first cycle the initial conditions are as follows:

$C_i(Z,0)=0$; $q_i(Z,0)=0$; $T(Z,0)=T_{feed}$

In PTSA process, regeneration step has countercurrent flow direction with adsorption step. So the initial condition for the adsorption step and final conditions of the regeneration steps (except for the first cycle) will be the same. In other words the initial conditions in succeeding cycles are as follows:

$C_i(Z,0)=C_i(Z', t_c)$; $q_i(Z,0)=q_i(Z',t_c)$; $T(Z,0)=T_{feed}$

The boundary conditions are as below:

$t>0 \quad Z=L \quad \frac{\partial C_i}{\partial Z}=0 \quad \frac{\partial T_i}{\partial Z}=0$

$Z=0 \; C_i=C_{i,feed}$; $P=P_{feed}$; $U=U_{feed}$; $T=T_{feed}$

3.5.2. Regeneration Step

In each cycle, depressurizing takes place before regeneration. As the variation of concentration and temperature at pressurizing and depressurizing steps are ignored, these two parameters will have the same values of those in the end of adsorption step (t_{ad}).

$C_i(Z',0)=C_i(Z, t_{ad})$; $q_i(Z',0)=q_i(Z,t_{ad})$; $T(Z',0)=T(Z, t_{ad})$

In regeneration step a purge gas free of adsorbing components has been used. So the boundary conditions are as following:

$t>0 \quad Z'=L \quad \frac{\partial C_i}{\partial Z}=0 \quad \frac{\partial T_i}{\partial Z}=0$

$Z'=0 \; C_i=0$; $P=P_{purge}$; $U=U_{purge}$; $T=T_{purge}$

3.6. Isotherm model

When an adsorbent comes in contact with the surrounding fluid having a certain composition, adsorption takes place and after a certain amount of time, the adsorbent and the surrounding fluid reach equilibrium condition. The curve illustrating the adsorption amount (q) versus the concentration of the fluid phase (C) is called adsorption isotherm. Usually the adsorption amounts are measured in constant temperature and the results are expressed by some mathematical equations called adsorption isotherm. According to adsorption process phenomena, a suitable adsorption isotherm model has to be incorporated. In PTSA process, temperature remains constant during adsorption while it varies a lot in regeneration step. Due to the large temperature variations during regeneration, the determined isotherm model shall include temperature dependent parameters. Therefore in current study for modeling of the mentioned PTSA process the extended Langmuir isotherm with temperature dependent parameters has been incorporated according to the following relation:

$$\frac{q_i}{q_i^*}=\frac{a_{1,i}*e^{\frac{a_{2,i}}{T}}*P_i}{1+\sum_k a_{3,k}e^{\frac{a_{4,i}}{T}}*P_k} \qquad (6)$$

The isotherm data for adsorption of water and mercaptan in vicinity of 13X Zeolite were obtained from literature [4,10]. The obtained data were then fitted according to the selected isotherm model (eq. 6) and finally the required parameters have been listed in Table 3.

The amounts of mercaptan and water adsorption heat on zeolite 13X are assumed to be 57.95 kj/mole and 75.6 kj/mol respectively.

Table 3. Isotherm constants of water and mercaptan adsorption on Zeolite 13X (based data is given from [4,10]

Parameter	Water	Mercaptan
a_1 (bar^{-1})	$7.654 * 10^{-4}$	$1.144 * 10^{-3}$
a_2 (k)	27555	2488
a_3 (bar^{-1})	$8.612 * 10^{-3}$	$9.155 * 10^{-4}$
a_4 (k)	2106	2574
q^*($kmol.kg^{-1}$)	$12.34 * 10^{-3}$	$11.87 * 10^{-3}$

3.7. Solution Technique for Model Equations

In order to solve the mentioned set of second and first order partial differential equations for each step of PTSA process, they have to be discrete by means of finite difference method. In present study, the bed length has been divided into 20 nodes and all the derivative terms ($\frac{\partial}{\partial Z}, \frac{\partial^2}{\partial Z^2}$) have been linear by the finite difference method. Time derivatives were left intact.

The resulting Differential-Algebraic equations (DAE's) had to be solved simultaneously. This was done by means of ode15s module in MATLAB software (version7.6).

4. Model Parameters Determination

4.1. Overall Mass Transfer Coefficient

The overall mass transfer coefficient ($K_{s,i}$) used in linear driving force (LDF) model (relation 3) can be expressed as a function of internal and external mass transfer coefficients in the following form[9]:

$$\frac{1}{K_{s,i}} = \frac{r_p}{3k_{f,i}} + \frac{r_p^2}{15\varepsilon_p D_{p,i}} \quad (7)$$

As shown in relation (7) above, the external mass transfer coefficient ($k_{f,i}$) and the effective diffusion coefficient of each component ($D_{p,i}$) shall be calculated to enable us obtain the overall mass transfer coefficient. So, to calculate the overall mass transfer coefficient, the following relations are applied:

- Binary molecular diffusion coefficient is calculated by the Wilke-Lee equation [11]:

$$D_{i,j} = 1.01 \times 10^{-4} \frac{T^{1.5}}{P\sigma_{i,j}^2 \Omega_D} \left(\frac{1}{M_i} + \frac{1}{M_j}\right)^{0.5} \left(0.0027 - 0.0005 \left(\frac{1}{M_i} + \frac{1}{M_j}\right)^{0.5}\right) \quad (8)$$

For estimation of Ω_D, an empirical correlation is used as following [12]

$$\Omega_D = \left(44.54 \left(\frac{kT}{\varepsilon_{i,j}}\right)^{-4.909} + 1.911 \left(\frac{kT}{\varepsilon_{i,j}}\right)^{-1.575}\right)^{0.1} \quad (9)$$

in which $\varepsilon = 0.841\ V_c^{1/3}$, $\varepsilon/k = 0.75\ T_c$ and $\varepsilon_{i,j} = (\varepsilon_i \varepsilon_j)^{0.5}$

- Molecular diffusion coefficient (D_m), Knudsen diffusion coefficient (D_K) and effective diffusion coefficient (D_P) in a gas mixture are calculated based on equations 10 to 12 [13]:

$$D_{m,i} = \left(\sum_{j=1, j\neq i}^{n} \frac{y_j}{D_{i,j}}\right)^{-1} \quad (10)$$

$$D_{k,i} = 9.7 \times 10^1 r_p \left(\frac{T}{M_i}\right)^{0.5} \quad (11)$$

$$D_{p,i} = \frac{1/\tau}{1/D_{m,i} + 1/D_{k,i}} \quad (12)$$

Torsion factor is calculated as below [14]:

$$\tau = \varepsilon_p + 1.5(1 - \varepsilon_p) \quad (13)$$

- The external film mass transfer coefficient is calculated by the following relation [15]:

$$N_{Sh} = \frac{k_{f,i} d_p}{D_{m,i}} = 2 + 1.1 Sc^{1/3} Re^{0.6} \quad (14)$$

4.2. Axial Dispersion Coefficient

Axial dispersion coefficient ($D_{z,i}$) is calculated by following relation [16]:

$$D_{z,i} = 0.73 D_{m,i} + \frac{Ur_p}{\varepsilon_p \left(1 + 9.49 \frac{\varepsilon_p D_{m,i}}{2Ur_p}\right)} \quad (15)$$

4.3. Physical Properties of the Gas

In order to solve the model equations, the values of the gas compressibility factor (z), viscosity (μ), Heat capacity (C_{pg}) and heat transfer coefficient (λ) have to be specified. Gas

compressibility factor is calculated by Peng-Robinson (PR) state equation. The other parameters of the gas phase (assuming methane as feed) are obtained from Aspen HYSYS software data bank [12] (Aspen HYSYS software ver. 7.3). Finally the temperature relations for every characteristics of the gas are fitted according to the equations described in Table 4.

Table 4. Gas property based on the function of temperature (based data is given from Aspen HYSYS Ver. 7.3)

Pressure = 10 Barg				
Function	a	b	c	d
C_{pg} (kj/kg.K)	$-1 * 10^{-8}$	$2*10^{-5}$	-0.0052	2.6651
λ (kj/m.s.K)	$-5 * 10^{-14}$	$1 * 10^{-10}$	$8 * 10^{-8}$	$1*10^{-6}$
μ (kg/m.s)	$2 * 10^{-14}$	$-5 *10^{-11}$	$6 * 10^{-8}$	$-1*10^{-6}$
Pressure = 67 Barg				
C_{pg} (kj/kg.K)	$-4*10^{-8}$	$6 *10^{-5}$	-0.0283	6.7639
λ (kj/m.s.K)	$-2 * 10^{-13}$	$-6 *10^{-8}$	$-6 *10^{-8}$	$3 *10^{-5}$
μ (kg/m.s)	$-2 * 10^{-14}$	$2 *10^{-8}$	$2 *10^{-8}$	$6 *10^{-6}$
$f=a*T^3+b*T^2+c*T+ d$; T(k)				

5. Results and Discussions

The simulation results have been reported for 3 cycles. According to process description, each cycle includes, adsorption step (18 hours) depressurizing step (half an hour), regeneration step (16 hours) and pressurizing step (half an hour).

5.1. Water Mole Fraction Profile

Figure 1 illustrates the mole fraction profile of water in gas phase at three different points of the bed. The results are obtained from simulation during three consecutive cycles (0-105 h).

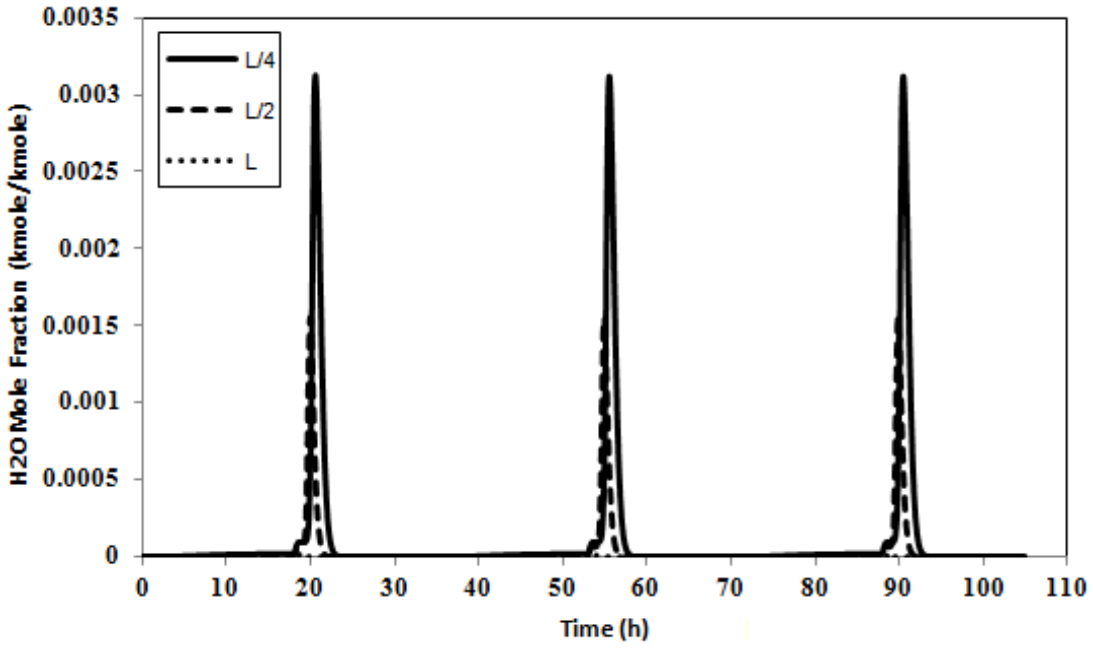

Figure 1. Mole fraction of water in gas phase, during of 3 consecutive cycle and at various points along the bed.

As shown in figure 1, after approximately 2 cycles (0-70 h), the difference between the mole fractions of water for the first and second cycle gets negligible. In other words the system reaches to steady state condition after two consecutive cycles.

This figure also shows that, during adsorption step of each cycle, the water content of gas, increases with time along the bed. It is also noticed from this figure that during adsorption step and at Z=L/4 & L/2, the water content of the gas increases to the point that it reaches the amount of the water content in the feed (bed will be saturated).

As mentioned, the regeneration gas flow direction is from bottom to the top of the bed. So during regeneration step, the water concentration decreases rapidly from the bottom of bed (Z=L).

Water mole fraction profiles for steady state condition and adsorption step in second cycle have been depicted in figure 2 (70-86 h). It can be seen from this figure that at different points of the bed, the water concentration increases by time. However the rate of this increase is not the same for all parts of the bed. In other words the water concentration of gas in the bed is decreased from first to last location of the bed.

At the end of adsorption step, (Z=0-L/2), the bed gets saturated with water (water amount gets equal to water concentration in the feed, $1.88*10^{-5}$), while the amount of water in the product gas (Z=L) is less than 1ppmv (0.26 ppmv)

The modeling prediction data for outlet water vapor composition in the product have been compared with the mentioned industrial unit data. The result show that mathematical modeling can predict outlet water vapor composition with high accuracy and there is good agreement between the modeling predictions and the mentioned industrial unit data (0.3 ppmv).

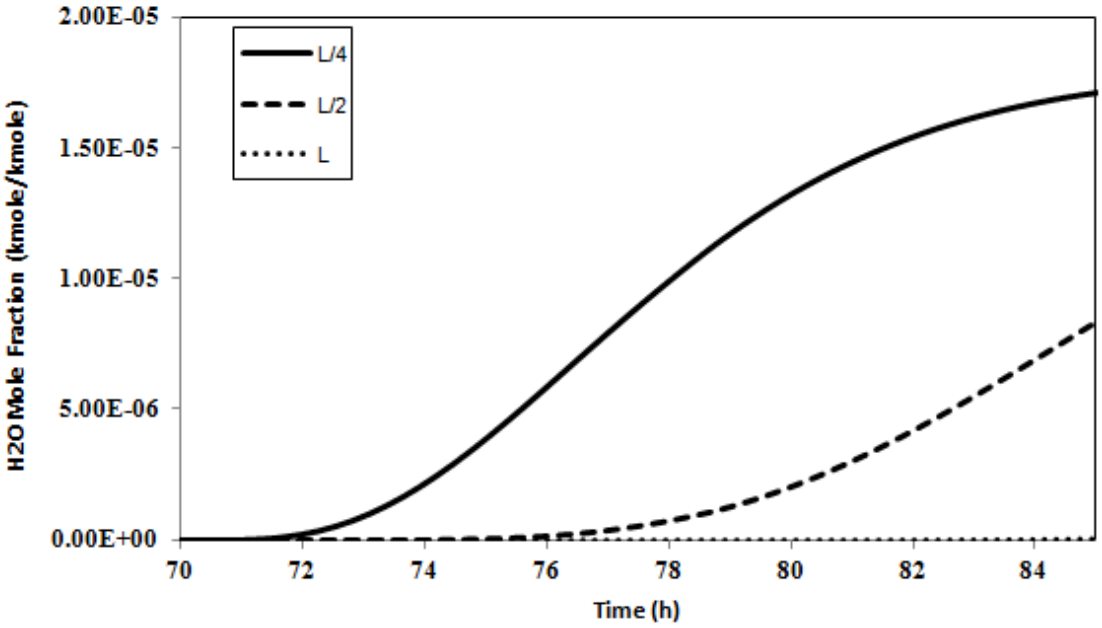

Figure 2. Mole fraction of water in gas phase along the bed at the adsorption step

5.2. Mercaptan Mole Fraction Profile

Figure 3 illustrates the mercaptan concentration variation along the bed for three consecutive cycles. According to the product specifications of the industrial unit under study, mercaptan content of the product is 5ppmv. The modeling results at end of adsorption step of second cycle, predicted the mercaptan content of the product to be 5.02 ppmv which is well in compliance with the experimental data. The results show that there is excellent agreement between model predictions and experimental data so the proposed model can predict the mercaptan and water content of product by high accuracy.

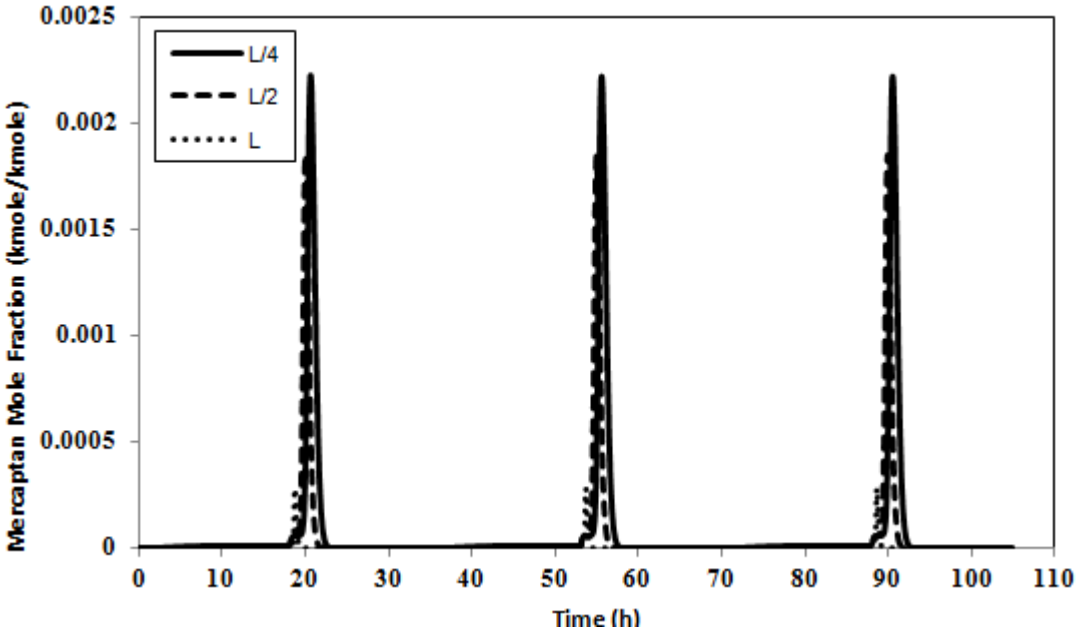

Figure 3. Mercaptan concentration profile at various points of adsorption bed.

Figure 4 shows the mercaptan concentration after steady state condition in adsorption step of second cycle. Comparing figures 2 and 4 shows that, the variation of mercaptan content at different points of the bed is similar to that of the water content. It is also noticed from these figures that mercaptan adsorption occurs more than that of water and so the bed gets saturated with mercaptan in a short period of time.

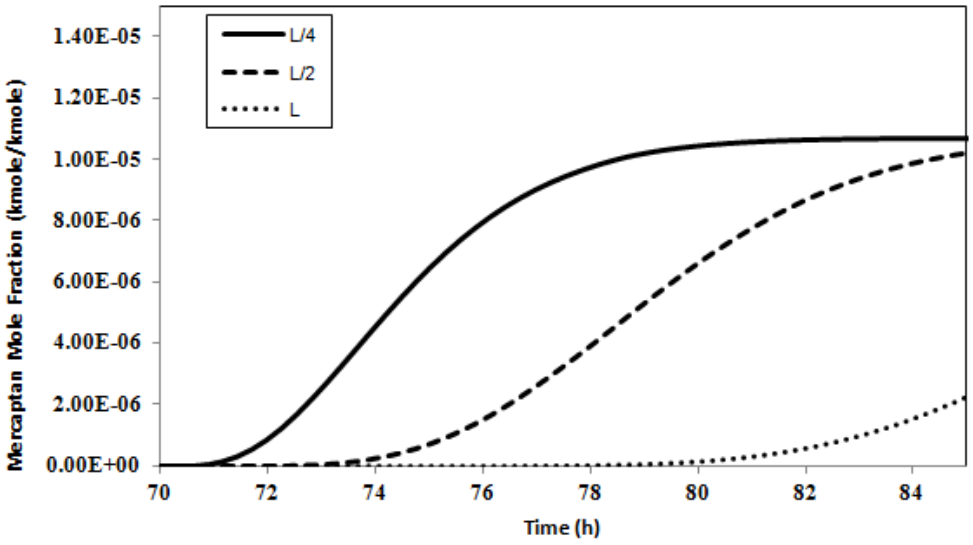

Figure 4. Mercaptan concentration profile in adsorption step along the bed

5.3. Temperature Profile of Adsorbent and Gas

As it is assumed that thermal equilibrium exists between the adsorbent and the gas phase, therefore the temperature profiles of the gas phase and adsorbent are the same. Figure 5 shows that the temperature variation of gas and adsorbent are approximately minor in adsorption step while it is tangible during regeneration.

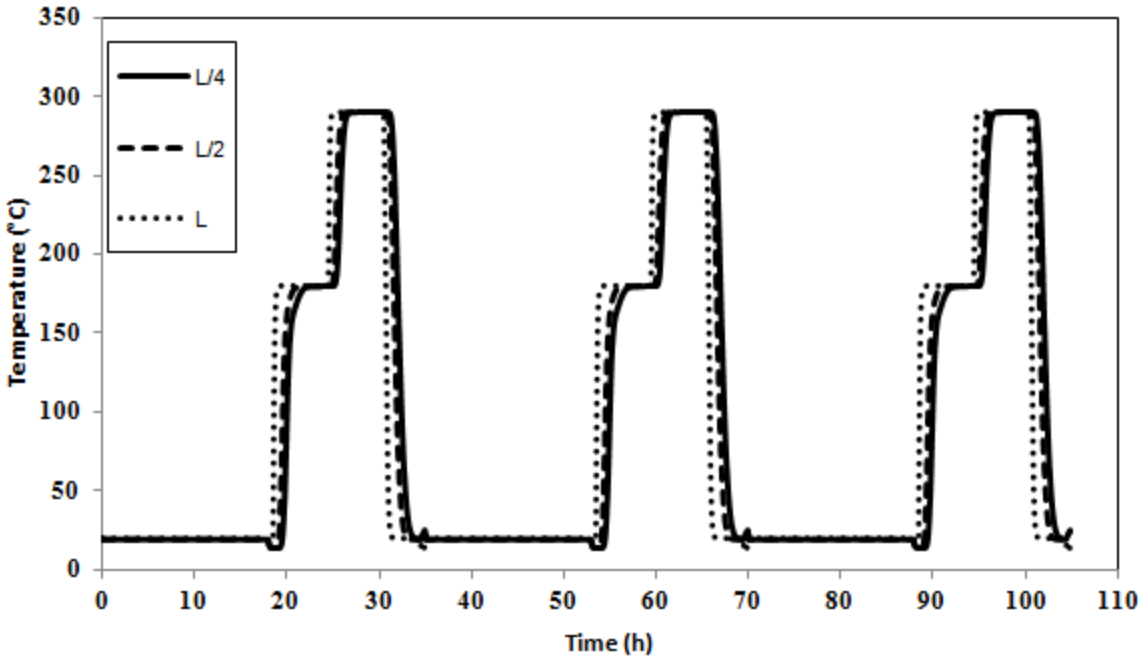

Figure 5. Temperature profile at various points of adsorption bed

6. Effects of operating parameters

The effects of process variables on the performance of the industrial unit under study were investigated using the simulation. Simulations were carried out by varying one parameter while keeping constant the others.

6.1. Operating Pressure

In order to investigate the effect of pressure on product quality, the operating pressure was changed from 50 to 70 bars, while all other operating conditions (Table 1, 2) were kept constant.

Table 5. Effect of feed pressure on the adsorption performance

Operating Pressure (bara)	Water content of Product (ppmv)	Mercaptan content of Product (ppmv)	Bed pressure loss (bar)
50	2.4	9.5	0.110
55	1.3	8.4	0.099
60	0.62	7	0.091
65	0.31	5.6	0.083
70	0.16	4.3	0.076

The results show that increase of feed pressure leads to bed pressure drop and hence decrease of water and mercaptan concentration of the product (table 5). This happens because the feed gas volume flow rate decreases with increase of the feed pressure while the other operating parameters are kept constant and so the gas contact time will increase.

6.2. Adsorbent Diameter

Figure 6 shows the variation of bed pressure drop and water & mercaptane content of the product versus adsorbent diameter. The particle diameters considered are 1.5×10^{-3}, 3.0×10^{-3} and 5.0×10^{-3}m. During these simulations other parameters such as flow rate, bed height, and inlet concentration are kept constant. It can be seen that increase of the adsorbent diameter in mentioned particle diameters have less effect on the water and mercaptan contents of the

produced gas. While the bed pressure drop is decreased with increasing of adsorbent diameter. According to Ergun equation, at constant bed porosity, increase of the adsorbent diameter will cause decrease of the bed pressure drop.

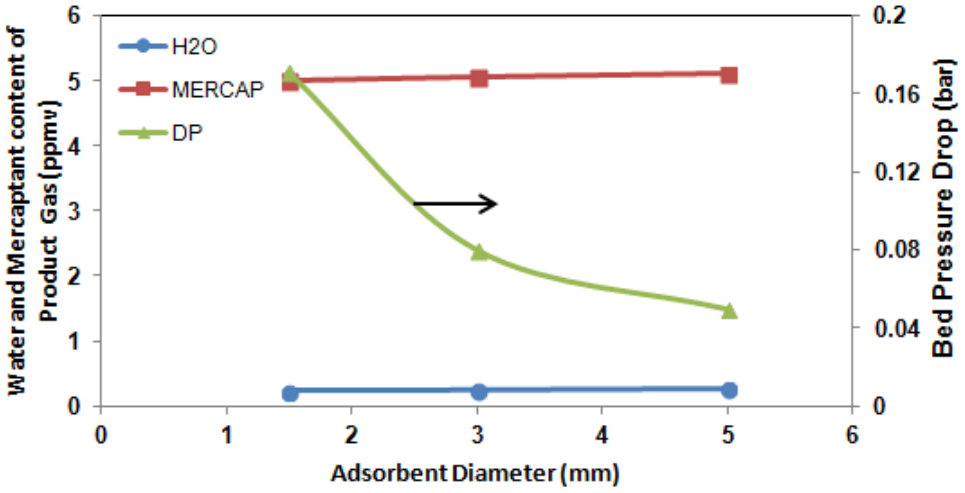

Figure 6. Effect of adsorbent diameter on the adsorption performance

6.3. Adsorption Temperature

The influence of adsorption temperature on the water & mercaptane concentrations in the product and the bed pressure drop is depicted in Figure 7. Since adsorption is an exothermic process, increase of the feed temperature will decrease the adsorption rates of water and mercaptan in the bed.

Also in constant feed pressure and molar flow rate, the gas volumetric flow rate increases by increase of the feed temperature. Therefore, gas space velocity in the bed will increase. For this reason the bed pressure drop will increase as well.

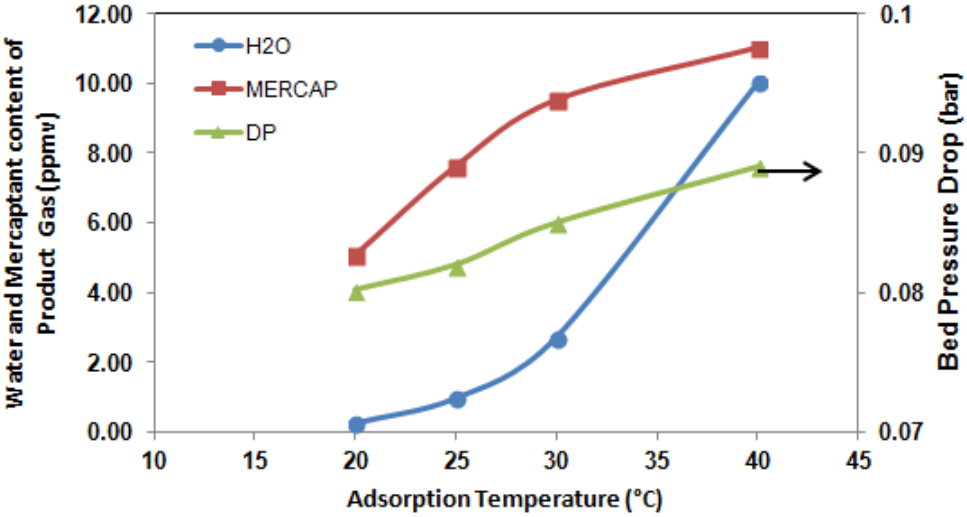

Figure 7. Effect of adsorption temperature on the adsorption performance

6.4. Regeneration Gas Flow Rate

The regeneration gas flow rate is determined by means of product specifications. Figure 8 illustrates the variations of water and mercaptan concentrations in product versus regeneration gas flow rate. In this study, the regeneration gas flow rate has been assumed to be 2, 3, 5 and 7 mole percent of the product flow.

As shown in figure 8, water and mercaptan concentrations of the produced gas decreases with increase of the regeneration gas flow rate. Also according to this figure, to obtain a suitable product in the industrial unit under study, the regeneration gas flow rate shall be at least 5 mole percent of the produced gas volume flow rate.

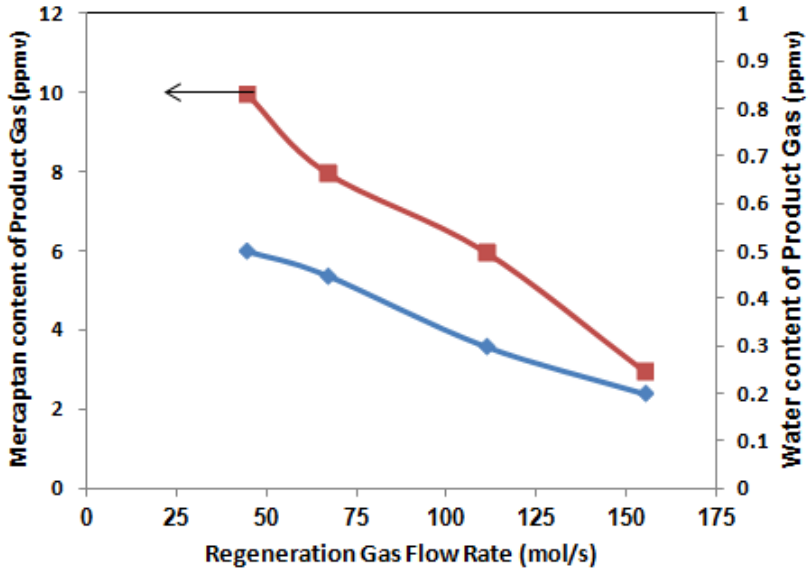

Figure 8. Effects of regeneration gas flow rate on the adsorption performance

7. Conclusions

In this work, based on a comprehensive mathematical model, an adsorption industrial unit (Gas Demercaptanization Unit) has been modeled by a computer programming in Matlab software.

The modeling results have been validated using the experimental data from the mentioned working industrial unit. Modeling studies are performed to investigate the effects of changing various process variables, such as operating pressure and temperature, adsorbent diameter and regeneration gas flow rate on the performance of the unit. The results showed that by increase of the adsorbent diameter and feed temperature, water and mercaptan content of the product will get decreased. On the other hand, increase of the adsorption pressure or regeneration gas flow rate will lead to decrease of the adsorbed components in the product.

Notation

C	*Component concentration (kmol/m^3)*
C_{pg}	*Gas heat capacity (kj/kg.k)*
C_{ps}	*Adsorbent heat capacity (kj/kg.k)*
d_p	*adsorbent diameter (m)*
$D_{p,I}$	*Effective diffusivity of component i(m^2/s)*
D_k	*Knudsen diffusion coefficient (m^2/s)*
D_m	*Molecular diffusion coefficient (m^2/s)*
D_z	*Axial dispersion coefficient (m^2/s)*
G	*Gas mass flow rate base on bed section area (kg/(m^2.s))*
H_i	*Adsorption heat of Component i (kj/kmol)*
$k_{f,I}$	*External mass transfer coefficient for Component i (m/s)*
$K_{s,I}$	*Overall mass transfer coefficient for Component i (1/s)*
L	*Bed length (m)*
M	*Molecular weight (kg/kmol)*
P_i	*Component i partial pressure (bar)*
P	*Gas pressure (bar)*
q_i	*Concentration of adsorbate i (kmol/kg)*

q_i^*	*Specific saturation adsorption capacity of compound i in the multisite Langmuir isotherm (kmol/kg)*
r_p	*Adsorbent radius (m)*
R	*Gas constant, 0.083145 (bar.m^3/kmol.k)*
$\mathrm{Re} = \frac{Gd_p}{\mu}$	*Reynolds number*
$Sc = \frac{\mu}{\rho_g D_{m,i}}$	*Schmitt number*
T	*Temperature (K)*
T_c	*Critical temperature (k)*
U	*Superficial gas Velocity (m/s)*
V_c	*Critical volume (m^3/kmol)*
y_i	*Mole fraction of component i*
z	*Gas compressibility factor*
Z	*Distance in the bed from the entrance of bed (m)*
Z'	*Distance in the bed from the existence of bed (m), Z'=L-Z*
E	*Bed porosity*
ε_p	*Adsorbent porosity*
μ	*Viscosity (kg/m.s)*
λ	Heat transfer coefficient *(kj/m.s.k)*
ρ_q	*Gas density (kg/m^3)*
ρ_p	*Adsorbent bulk density (kg/m^3)*
$\sigma_{l,j}$	*(A) ‘* $\sigma_{l,j} = \frac{\sigma_i + \sigma_j}{2}$
T	*Tortuosity factor*

References

[1] Kidnay J, Parrish WR. 2006. Fundamentals of Natural Gas Processing, Taylor and Francis Group.

[2] Ruthven DM. 1984. Principles of adsorption and adsorption processes, John Wiley & Sons, New York

[3] Wakita H, Tachibana Y, Hosaka M. 2001. Removal of dimethyl sulfide and t-butyl-mercaptan from city gas by adsorption on zeolites. Microporous and Mesoporous Materials. 46, 237-247.

[4] Weber G, Benoit F, Bellat J, Paulin C, Mougin P, Thomas M. 2008. Adsorption equilibria of binary ethylmercaptan/hydrocarbon mixtures on a NaX zeolite. Micro-porous and Mesoporous Material. 109, 184-192.

[5] Tamai H, Nagoya H, Shiho T. 2006. Adsorption of methyl mercaptan on surface modified activated carbon. Journal of Colloid and Interface Science. 300, 814-817.

[6] Esmaili Dj, Ehsani M. 2008. Simulation of mercaptan removal from natural gas by using of adsorbent 13X in the constant temperature: Presented in Zeolite Interna-tional Conference, Iran.

[7] Shirani B, Kaghazch, T, Beheshti M. 2010. Water and mercaptan adsorption on 13X zeolite in natural gas purification process. Korean J. Chem. Eng. 27(1), 253-260.

[8] Green D, Perry R. 2007. Perry’s Chemical Engineering’s’ Handbook, 8th ed., McGraw-Hill, New York

[9] Yang RT. 1987. Gas separation by adsorption processes, Butterworth, Stoneham

[10] Ferreira D, Magalhaes R. 2011. Effective adsorption equilibrium isotherms and breakthroughs of water vapor and carbon dioxide on different adsorbent. Industrial Engineering and Chemical Research. 50, 10201-10210.

[11] Wilke CR, Lee CY. 1995. Ind. Eng. Chem. 47, 1253-1257

[12] Suzuki M. 1990. Adsorption Engineering, Chemical Engineering Monographs, Else-vier, Tokyo.

[13] Bird RB, Stewart WE, Lightfoot EN. 2002. Transport Phenomena, 2nd. ed., Wiley, New York.
[14] Suzuki M, Smith JM. 1972. Axial Dispersion in Beds of Small Particles. Chem. Eng. Sci. 3, 256-264.
[15] Jee JG, Kim MB, Lee CH. 2001. Adsorption characteristics of hydrogen mixtures in a layered bed: binary, ternary and five component mixtures. Ind. Eng. Chem. Res. 40, 868-878.
[16] Kast VW. 1988. Adsorption aus der Gasphase, VCH, Weinheim.
[17] Aspen HYSYS Software, Version 7.3,2011, Aspen Technology Inc.
[18] Park JH, Kim JN, Cho SH, Kim JD, Yang RT. 1998. Adsorber dynamics and optimal design of layered beds for multicomponent gas adsorption. Chem. Eng. Sci. 53(23), 3951-3963.

Corresponding author: Fax: (0098)21-44739716, E-mail: sadeghzadehj@ripi.ir